

Heavy ion beam probe operation in time varying equilibria of improved confinement reversed field pinch discharges

D. R. Demers, X. Chen, P. M. Schoch, and P. J. Fimognari

Citation: *Rev. Sci. Instrum.* **81**, 10E109 (2010); doi: 10.1063/1.3479109

View online: <http://dx.doi.org/10.1063/1.3479109>

View Table of Contents: <http://rsi.aip.org/resource/1/RSINAK/v81/i10>

Published by the [American Institute of Physics](http://www.aip.org).

Additional information on *Rev. Sci. Instrum.*

Journal Homepage: <http://rsi.aip.org>

Journal Information: http://rsi.aip.org/about/about_the_journal

Top downloads: http://rsi.aip.org/features/most_downloaded

Information for Authors: <http://rsi.aip.org/authors>

ADVERTISEMENT

physicstoday

Comment on any
Physics Today article.

Measured energy in Japan
David von Seggern
(vonseg@seismo.unr.edu) University of Nevada
July 2012, page 10
DIGITAL OBJECT IDENTIFIER
<http://dx.doi.org/10.1063/PT.3.1619>

Comment on this article
By the act of hitting a ball with a bat, one calculates the force energy to deliver the ball to its new location, but one must also take into account that the ball extended its energy release to that which became struck by the ball as its momentum ceased and passed energy to the struck team. Therefore the parameters of the damage extend into the future when the received energy to that pushed upon, later becomes released in a new event. Perhaps calculations of one added that in while another's calculations did not. E.M.C.
Written by Edgar Mocarvill, 14 July 2012 19:59

Heavy ion beam probe operation in time varying equilibria of improved confinement reversed field pinch discharges^{a)}

D. R. Demers,¹ X. Chen,¹ P. M. Schoch,¹ and P. J. Fimognari²

¹*Rensselaer Polytechnic Institute, Troy, New York 12180, USA*

²*University of Wisconsin, Madison, Wisconsin 53706, USA*

(Presented 19 May 2010; received 15 May 2010; accepted 7 July 2010;
published online 6 October 2010)

Operation of a heavy ion beam probe (HIBP) on a reversed field pinch is unique from other toroidal applications because the magnetic field is more temporal and largely produced by plasma current. Improved confinement, produced through the transient application of a poloidal electric field which leads to a reduction of dynamo activity, exhibits gradual changes in equilibrium plasma quantities. A consequence of this is sweeping of the HIBP trajectories by the dynamic magnetic field, resulting in motion of the sample volume. In addition, the plasma potential evolves with the magnetic equilibrium. Measurement of the potential as a function of time is thus a combination of temporal changes of the equilibrium and motion of the sample volume. A frequent additional complication is a nonideal balance of ion current on the detectors resulting from changes in the beam trajectory (magnetic field) and energy (plasma potential). This necessitates use of data selection criteria. Nevertheless, the HIBP on the Madison Symmetric Torus has acquired measurements as a function of time throughout improved confinement. A technique developed to infer the potential in the improved confinement reversed field pinch from HIBP data in light of the time varying plasma equilibrium will be discussed. © 2010 American Institute of Physics. [doi:10.1063/1.3479109]

I. INTRODUCTION

Operation of a heavy ion beam probe (HIBP) on a reversed field pinch (RFP) presents unique challenges. The most fundamental issue is accurate prediction of the beam trajectory and sample volume for each plasma discharge. The HIBP discussed in this article is installed on the Madison Symmetric Torus¹ (MST); unlike many other magnetic confinement configurations, the fields in MST are produced by currents driven in the toroidal vacuum chamber and the plasma. Magnetic field reconstruction, via equilibrium modeling constrained with diagnostic data, is performed after a discharge has occurred. A supplemental issue arising from the generation of magnetic field by currents in the vacuum chamber is a restriction on diagnostic port size. Small ports necessitate cross-over electrostatic beam steering systems to achieve desired beam injection and detection angles. Large ports increase the local magnetic field errors that must be taken into account when computing beam trajectories. Port sizes also affect the levels and consequences of ultraviolet radiation and particles streaming from the plasma into the beamlines.²

Two RFP discharge types (loosely comparable to H- and L-modes in tokamaks) are improved and standard confinement. Improved confinement discharges are achieved by application of inductive pulsed poloidal current drive (PPCD), which provides a supplementary poloidal electric field, and result in temporal evolution of the magnetic field.^{3,4} This

alteration of the magnetic equilibrium effectively sweeps the beam trajectories and thus the sample volumes in the plasma. In addition, the plasma potential evolves with the magnetic equilibrium. These PPCD discharge features will be considered throughout the remainder of this article. If beam injection energy and angle are held constant, the sample volume in the plasma moves as a function of time in concert with the temporal changes of the equilibrium. Standard discharges exhibit dynamo reconnection events that alter the magnetic equilibrium and thus beam trajectory, but will not be discussed here. Regardless of discharge type, HIBP operation in a RFP requires temporal reconstructions of magnetic equilibrium which are used to compute beam trajectories and to infer the motion and location of the sample volume in the plasma. This simulation and selection process permits a temporal and spatial mapping of the electric plasma potential in the RFP.

II. THE HEAVY ION BEAM PROBE ON MST

A 200 keV accelerator and an electrostatic energy analyzer⁵ are used to produce and detect the singly and doubly charged ion beams, respectively. The comparable magnitudes of the toroidal and poloidal magnetic fields of MST result in three dimensional beam trajectories. This feature, combined with the small diagnostic ports, necessitates steering of the ion beam in the primary (injection) and secondary (detection) beamlines. A unique cross-over type system was designed to enable beam injection into MST at angles of $\pm 20^\circ$ radially and $\pm 5^\circ$ toroidally through a very small port, and a triplet of steering elements to redirect the secondary

^{a)}Contributed paper, published as part of the Proceedings of the 18th Topical Conference on High-Temperature Plasma Diagnostics, Wildwood, New Jersey, May 2010.

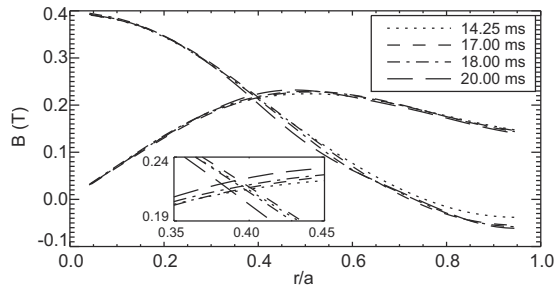


FIG. 1. Reconstructed PPCD magnetic equilibrium profiles of B_θ and B_ϕ at four time points relative to plasma discharge start time.

beam into the energy analyzer. Detailed descriptions of the HIBP on MST may be found in previous publications.^{6,7}

III. HIBP TRAJECTORIES IN IMPROVED CONFINEMENT RFP DISCHARGES

PPCD discharges in MST, produced through the transient application of a poloidal electric field which leads to a reduction of dynamo activity, result in the onset of an improved confinement period that occurs between 13 and 23 ms.⁸ A 365 kA PPCD plasma (shot 1090612094) with a density of 0.5×10^{19} cm³ will be used throughout this discussion. It rotates relative to the vacuum chamber and has low amplitude magnetic modes.⁹ During the improved confinement period, the data acquired by the HIBP are well balanced on two detector sets and suitable for the illustration of simultaneous and spatial measurement comparisons. Six points in time, distributed throughout improved confinement, are used to illustrate the temporal change in the magnetic field and consequential effect on the HIBP trajectory. Figure 1 shows the equilibrium profiles of B_θ and B_ϕ produced using MSTfit (Ref. 10) (an equilibrium reconstruction program) at four of these times relative to the start ($t=0$) of the discharge.

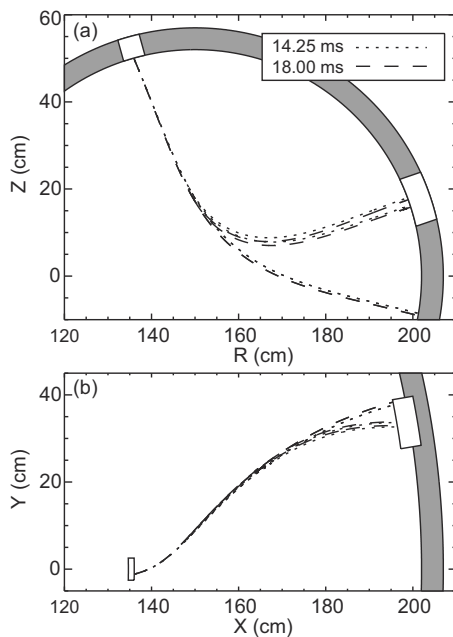


FIG. 2. (a) Poloidal and (b) toroidal projections of primary and secondary trajectories corresponding to magnetic equilibria shown in Fig. 1.

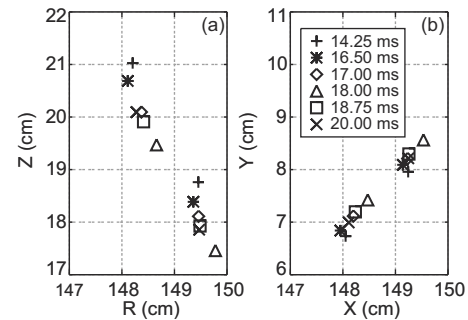


FIG. 3. Sample volume midpoints ($Z \sim 20$, $Y \sim 7$) and ($Z \sim 18$, $Y \sim 8.3$) that map to the center and top detectors, respectively, at six points in time.

Local changes in the magnetic profiles are modest, but the cumulative effect on the path of the ion beam is significant.

Figure 2 shows (a) poloidal and (b) toroidal projections of the primary and secondary ion trajectories of a 45 keV K^+ beam injected (at X, Y, Z) = (136, -1, 50 cm) with a fixed angle into the plasma for the magnetic equilibria reconstructed for 14.25 and 18.0 ms. Electron impact ionization of the primary beam produces a spray of secondary ions which are deflected and shown exiting through the port at the right hand side of the figures. The use of an analyzer with multiple apertures enables simultaneous measurements from spatially distinct sample volumes. The pairs of secondaries shown map onto the center and top detectors within the analyzer. Figure 3 shows the sample volume midpoints that map to the detectors for six points (magnetic equilibrium) in time during this discharge. Unlike many other magnetic confinement configurations, they have three dimensional displacements as a function of time. The motion of the center detector sample volume ($Z=19.5-21$, $Y=6.7-7.4$) is 1.6 cm between 14.25 and 18 ms (and can be considerably larger in other PPCD discharges). A notable temporal effect of the magnetic profile evolution is the sweeping of the sample volume inward in Z (from 14.25 to 18.0 ms) and then outward (from 18.0 to 20.0 ms).

IV. POTENTIAL MEASUREMENT

This PPCD discharge has a moderate period of improved confinement; features of reduced magnetic stochasticity are not fully evident before 16 ms. Figure 4 illustrates the secondary ion signals acquired simultaneously by the center and top detectors throughout the PPCD phase. Figures (a) and (b)

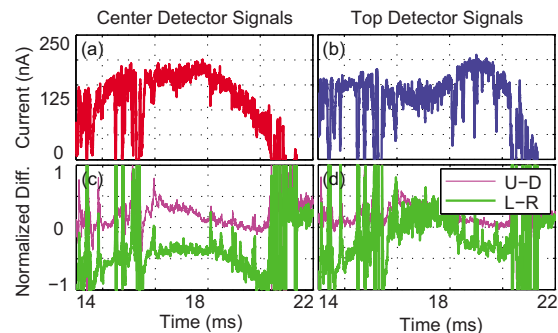


FIG. 4. (Color online) Simultaneously measured sum [(a) and (b)] and difference [(c) and (d)] illustrate total current and balance as a function of time.

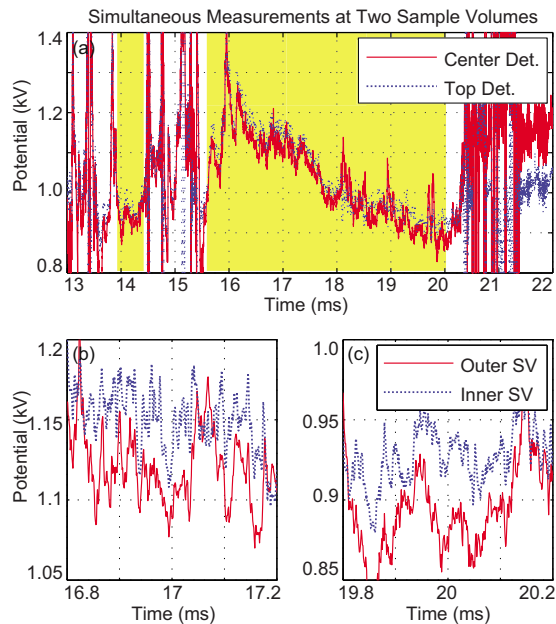


FIG. 5. (Color online) The electric potential (highlighted bands illustrate periods when most inferences are reliable) calculated using data shown in Fig. 4.

show the sum of the secondary ion current measured by each detector comprised of four plates; Figs. (c) and (d) show the upper two plates (U) minus the lower (D), and left two (L) minus the right plate (R) currents normalized by each sum signal. The distribution of the ion current on the detectors is important because uncertainty in the measured potential decreases when the sum signal is large, and when the signal is balanced, i.e., (U–D) and (L–R) are close to zero.¹¹ Nonideal current balance is a challenge of measurements during PPCD; the simultaneous sum and difference profiles illustrate this issue and the necessity of data selection criteria.

The variation in the center and top detector signal features is dominated by the changing magnetic equilibrium and electric potential of the plasma (which alter the beam trajectories through the plasma and secondary beamline, and deflection by the analyzer).¹² The temporal evolution of the equilibrium and trajectory during improved confinement prompts consideration of two issues when measuring the electric potential: (a) Is there a gradient in the plasma, and if so will motion of the sample volume across it mimic a local change in potential as a function of time? and (b) Is the local potential changing, but is it difficult to identify due to sample volume motion? These issues may be addressed using (1) accurate reconstructed magnetic equilibrium and sample volumes and (2) simultaneous measurements at two sample volumes that are swept with time during a single discharge. Using the foundation for (1) which was established in Sec. III, and the data to address (2) which is presented in Fig. 4, we provide in the following paragraphs the answer to (a) and (b) there is a potential gradient in the plasma and the local potential is changing. Thus, we demonstrate the establishment of a technique to infer the potential with a HIBP in the improved confinement RFP.

Figure 5(a) shows the electric potential of the plasma measured simultaneously by the top and center detectors (calculated using the data shown in Fig. 4). The potential at 16.5 ms is ~ 1.1 kV shortly after the onset of improved confinement. The highlighted bands illustrate periods during which most secondary ion signals are suitable for this measurement; large excursions in the sum or difference in Fig. 4 will not produce accurate potential. These data correspond to the sample volumes that vary in space with time as shown in Fig. 3; data from the center detector map to larger radii ($\rho = 19.5\text{--}21.1$) and the top detector to those closer to the core ($\rho = 17.5\text{--}18.8$). Figures 5(b) and 5(c) zoom in on 0.4 ms to illustrate that the magnitudes at the inner sample volume are larger than that at the outer which implies existence of a potential gradient. Using the data in Fig. 5(b) and the 2 cm spacing between sample volumes at 17 ms, we estimate a local outwardly directed radial electric field of 2.25 kV/m; the average electric field (relative to the plasma edge) is ~ 3.5 kV/m implying the existence of stronger fields further out in radius. To ascertain if the potential is decreasing as a function of time, as it appears in Fig. 5(a), we compare the measurements from the center detector at 17 and 20 ms, which map to proximal sample volumes (as shown in Fig. 3). The approximate values are 1.1 and 0.9 kV, respectively, implying that the local potential has indeed decreased as a function of time. This may suggest a mitigated loss of electrons due to a reduction of magnetic stochasticity during improved confinement.

PPCD quality and characteristics are highly variable. Ongoing analysis is necessary to confirm these inferences.

ACKNOWLEDGMENTS

This work was supported by U.S. DOE.

- ¹R. N. Dexter, D. W. Kerst, T. W. Lovell, S. C. Prager, and J. C. Sprott, *Fusion Technol.* **19**, 131 (1991).
- ²D. R. Demers, K. A. Connor, J. Lei, P. M. Schoch, and U. Shah, *Rev. Sci. Instrum.* **72**, 568 (2001).
- ³J. S. Sarff, N. E. Lanier, S. C. Prager, and M. R. Stoneking, *Phys. Rev. Lett.* **78**, 62 (1997).
- ⁴B. E. Chapman, A. F. Almagri, J. K. Anderson, T. M. Biewer, P. K. Chattopadhyay, C.-S. Chiang, D. Craig, D. J. Den Hartog, G. Fiksel, C. B. Forest, A. K. Hansen, D. Holly, N. E. Lanier, R. O'Connell, S. C. Prager, J. C. Reardon, J. S. Sarff, M. D. Wyman, D. L. Brower, W. X. Ding, Y. Jiang, S. D. Terry, P. Franz, L. Marrelli, and P. Martin, *Phys. Plasmas* **9**, 2061 (2002).
- ⁵T. S. Green and G. A. Proca, *Rev. Sci. Instrum.* **41**, 1409 (1970).
- ⁶J. Lei, U. Shah, D. R. Demers, K. A. Connor, and P. M. Schoch, *Rev. Sci. Instrum.* **72**, 564 (2001).
- ⁷J. Lei, T. P. Crowley, U. Shah, P. M. Schoch, K. A. Connor, and J. Schatz, *Rev. Sci. Instrum.* **70**, 967 (1999).
- ⁸J. K. Anderson, J. Adney, A. Almagri *et al.*, *Phys. Plasmas* **12**, 056118 (2005).
- ⁹A. F. Almagri, S. Assadi, S. C. Prager, J. S. Sarff, and D. W. Kerst, *Phys. Fluids B* **4**, 4080 (1992).
- ¹⁰J. K. Anderson, C. B. Forest, T. M. Biewer, J. S. Sarff, and J. C. Wright, *Nucl. Fusion* **44**, 162 (2004).
- ¹¹L. Solensten and K. A. Connor, *Rev. Sci. Instrum.* **58**, 516 (1987).
- ¹²D. R. Demers, X. Chen, P. M. Schoch, and P. J. Fimognari, *Proceedings of the 50th Annual Meeting of the DPP*, Dallas, TX, 2008, (American Physical Society, College Park, MD, 2008), Vol. 53, No. 14, p. 183.